

Prototype-Guided Diffusion: Visual Conditioning without External Memory

Bilal FAYE¹, Hanane AZZAG², Mustapha Lebbah³
 e-mail: faye@lipn.univ-paris13.fr, azzag@univ-paris13.fr, mustapha.lebbah@uvsq.fr

Abstract—Diffusion models have emerged as a leading framework for high-quality image generation, offering stable training and strong performance across diverse domains. However, they remain computationally intensive, particularly during the iterative denoising process. Latent-space models like Stable Diffusion alleviate some of this cost by operating in compressed representations, though at the expense of fine-grained detail. More recent approaches such as Retrieval-Augmented Diffusion Models (RDM) address efficiency by conditioning denoising on similar examples retrieved from large external memory banks. While effective, these methods introduce drawbacks: they require costly storage and retrieval infrastructure, depend on static vision-language models like CLIP for similarity, and lack adaptability during training. We propose the *Prototype Diffusion Model (PDM)*, a method that integrates prototype learning directly into the diffusion process for efficient and adaptive visual conditioning—without external memory. Instead of retrieving reference samples, PDM constructs a dynamic set of compact visual prototypes from clean image features using contrastive learning. These prototypes guide the denoising steps by aligning noisy representations with semantically relevant visual patterns, enabling efficient generation with strong semantic grounding. Experiments show that PDM maintains high generation quality while reducing computational and storage overhead, offering a scalable alternative to retrieval-based conditioning in diffusion models. Our code is publicly available at <https://github.com/b-faye/pdm>.

I. INTRODUCTION

Diffusion models have rapidly emerged as a dominant class of generative models, known for their high sample quality, training stability, and flexibility across diverse tasks. Since the introduction of Denoising Diffusion Probabilistic Models (DDPMs) [1], subsequent works have demonstrated their superiority over GAN-based approaches [2, 3]. These models have since been extended to tasks such as unconditional generation [4], super-resolution [5], inpainting [6], and notably, text-to-image generation [7, 8]. Despite their effectiveness, diffusion models are notoriously slow at both training and inference, owing to the iterative nature of the denoising process. To mitigate this, models such as Stable Diffusion [8] propose operating in a learned latent space, significantly reducing computational requirements. However, this efficiency comes at the cost of fine spatial details and often requires powerful encoders and decoders to preserve semantic fidelity.

More recently, methods such as Retrieval-Augmented Diffusion Models (RDM) [9] aim to condition the denoising process using external visual memories. By retrieving semantically similar image patches or examples via pretrained vision-language models (e.g., CLIP [10]), RDM

dynamically steers generation toward more contextually relevant outputs. While this improves controllability and speeds up convergence, it introduces dependencies on large-scale memory banks and fixed feature extractors. These limitations raise concerns regarding memory cost, system latency, and adaptability during training.

An orthogonal line of work—ProtoDiffusion [11]—attempts to incorporate prototype learning into diffusion training by precomputing class-specific prototypes and using them as conditioning embeddings. Though effective in accelerating convergence, this two-stage approach decouples prototype learning from diffusion training, leading to rigidity in prototype representations and a lack of adaptability to evolving feature distributions. Moreover, class-level conditioning limits scalability in fine-grained or multimodal settings such as text-to-image generation.

We introduce the *Prototype Diffusion Model (PDM)*, a unified framework that integrates online prototype learning into the diffusion training loop for efficient, context-aware generation—without relying on external memory or fixed embeddings. In contrast to RDM, our model dynamically constructs prototypes from clean intermediate features using contrastive objectives, and reuses them as visual anchors during the noisy denoising steps. Unlike ProtoDiffusion, our prototypes are learned jointly and continuously, adapting to the evolving feature space throughout training. This tightly-coupled prototype-guided mechanism enhances semantic grounding while maintaining efficiency. Our contributions are:

- We propose a novel prototype-guided conditioning mechanism for diffusion models that avoids reliance on external retrieval systems or pretrained vision-language encoders.
- Our method enables joint prototype learning and generation, allowing prototypes to adapt dynamically during training rather than relying on static pretraining.
- We demonstrate that PDM matches or exceeds the generation quality of retrieval-augmented methods while significantly reducing memory overhead and inference latency.
- We validate our approach on conditional image generation benchmarks, showing consistent gains in quality and speed compared to both retrieval-based and prototype-initialized baselines.

II. RELATED WORK

A. Diffusion Models

Diffusion models have emerged as a leading paradigm in generative modeling, delivering strong performance in tasks such as image generation, inpainting, super-resolution, and text-to-image synthesis. Following the foundational Denoising Diffusion Probabilistic Models (DDPMs) by Ho et al. [1], numerous advances have improved their training stability and sample quality. Latent Diffusion Models (LDMs) [8] reduce the computational load by operating in compressed latent spaces, enabling high-resolution synthesis with fewer resources. Further refinements such as consistency models [12] and SDXL [13] have demonstrated the scalability and expressiveness of diffusion-based generation. Nonetheless, the denoising process remains inherently slow due to the requirement for hundreds of sequential steps, making inference expensive. While latent-space methods partially alleviate this, they often compromise spatial detail and semantic fidelity. To address these shortcomings, researchers have proposed leveraging external context to augment and guide the denoising trajectory.

B. Retrieval-Augmented Diffusion Models

Retrieval-augmented approaches aim to improve generation quality and speed by incorporating semantically relevant information retrieved from external memory banks. Blattmann et al. [9] introduced Retrieval-Augmented Diffusion Models (RDMs), which retrieve contextually similar image patches to guide the diffusion model using CLIP-based feature alignment. Similarly, IRDiff [14] demonstrates retrieval-augmented molecular generation by retrieving known protein-ligand interactions, improving data efficiency and generalization. These methods enable controllable generation and reduce the burden on the denoiser by introducing external visual priors. However, they introduce new challenges: dependence on large, static memory systems, high retrieval latency, and limited adaptability to evolving feature distributions. Moreover, reliance on frozen pretrained encoders (e.g., CLIP [10]) constrains the flexibility of conditioning and may cause semantic mismatches between the prompt and retrieved examples. These limitations motivate internal memory mechanisms that can offer similar semantic grounding without relying on costly retrieval infrastructure.

C. Prototype Learning in Diffusion Models

Prototype learning provides a compact and interpretable alternative for guiding generative models without external databases. Baykal et al. [11] proposed ProtoDiffusion, incorporating class-specific prototypes as conditioning inputs to accelerate convergence and improve semantic alignment. However, their two-stage framework learns prototypes independently from the diffusion process, resulting in rigid, static prototypes that may fail to capture evolving feature distributions during training. In few-shot and continual learning contexts, Du et al. [15]

and Doan et al. [16] introduced task-adaptive prototypes and class-conditioned diffusion to mitigate domain shifts and forgetting. While these approaches support dynamic conditioning, they either focus on discriminative tasks or rely on coarse, class-level prototypes—limiting fine-grained generation control and adaptability. Crucially, existing methods do not fully integrate prototype learning within the diffusion process itself.

Our proposed Prototype Diffusion Model (PDM) addresses this gap by introducing a fully joint training framework where patch-level prototypes are learned online from clean features and used to guide noisy denoising steps through a contrastive alignment objective. This enables PDM to maintain semantic consistency, support fine-grained conditioning, and reduce reliance on external memory—all while adapting prototypes dynamically throughout training.

III. BACKGROUND

A. Diffusion Models

Diffusion models are a class of generative models that learn to synthesize data by inverting a stochastic noising process. A prominent and widely used variant is the *Denoising Diffusion Probabilistic Model* (DDPM) [1, 17], which formulates generation as the reversal of a predefined forward diffusion process.

The forward process gradually corrupts a clean data sample $x_0 \in \mathbb{R}^d$, drawn from an unknown data distribution $q(x_0)$, by adding Gaussian noise over T discrete timesteps. This results in a sequence of latent variables x_1, \dots, x_T , defined recursively by:

$$q(x_t | x_{t-1}) = \mathcal{N}(x_t; \sqrt{1 - \beta_t} x_{t-1}, \beta_t \mathbf{I}), \quad (1)$$

where $\beta_t \in [0, 1]$ is a variance schedule controlling the amount of noise injected at each timestep, and \mathbf{I} is the identity matrix.

By defining $\alpha_t = 1 - \beta_t$ and the cumulative product $\bar{\alpha}_t = \prod_{s=1}^t \alpha_s$, the marginal distribution of x_t given x_0 admits a closed-form expression:

$$x_t = \sqrt{\bar{\alpha}_t} x_0 + \sqrt{1 - \bar{\alpha}_t} \epsilon, \quad \epsilon \sim \mathcal{N}(0, \mathbf{I}). \quad (2)$$

The goal of the model is to learn the reverse process $p_\theta(x_{t-1} | x_t)$, which is intractable in general. DDPM approximates this reverse process by a parameterized Gaussian distribution:

$$p_\theta(x_{t-1} | x_t) = \mathcal{N}(x_{t-1}; \mu_\theta(x_t, t), \Sigma_t), \quad (3)$$

where the mean $\mu_\theta(x_t, t)$ is predicted by a neural network and the variance Σ_t is typically fixed or learned.

A common parameterization predicts the noise ϵ added during the forward process. The mean of the reverse distribution is then recovered as:

$$\mu_\theta(x_t, t) = \frac{1}{\sqrt{\alpha_t}} \left(x_t - \frac{1 - \alpha_t}{\sqrt{1 - \bar{\alpha}_t}} \epsilon_\theta(x_t, t) \right), \quad (4)$$

where $\epsilon_\theta(x_t, t)$ is the model's estimate of the noise component ϵ at timestep t .

The model is trained to minimize the expected mean squared error between the true noise ϵ and the predicted noise ϵ_θ , resulting in the simplified training objective:

$$\mathcal{L}_{\text{simple}} = \mathbb{E}_{t, x_0, \epsilon} \left[\left\| \epsilon - \epsilon_\theta \left(\sqrt{\bar{\alpha}_t} x_0 + \sqrt{1 - \bar{\alpha}_t} \epsilon, t \right) \right\|^2 \right]. \quad (5)$$

This objective encourages the model to accurately denoise corrupted inputs at arbitrary timesteps, ultimately enabling sampling by iteratively denoising from pure Gaussian noise $x_T \sim \mathcal{N}(0, \mathbf{I})$ back to a coherent data sample x_0 .

B. Retrieval-Augmented Diffusion Models

Retrieval-Augmented Diffusion Models (RDMs) enhance classical diffusion models by incorporating a retrieval mechanism that conditions generation on external, real examples. This semi-parametric approach supplements the learned generative model with non-parametric memory, enabling improved sample diversity, controllability, and generalization [8, 9, 18].

Given an input image x , its latent representation $z = E(x)$ is computed using a pretrained encoder E , typically from an autoencoder such as VQ-GAN [19]. A forward diffusion process is then applied in the latent space to produce noisy samples z_1, \dots, z_T , analogous to the DDPM framework.

To enrich the generative process with semantic context, a retrieval function $\xi_k(x, D)$ selects the k nearest neighbors of x from a dataset D , based on similarity in a learned embedding space. This embedding space is induced by a pre-trained model ϕ , such as CLIP [10], and the retrieval is defined as:

$$\xi_k(x, D) = \text{Top-}k \left(\text{sim}(\phi(x), \phi(y)) \mid y \in D \right), \quad (6)$$

where $\text{sim}(\cdot, \cdot)$ denotes a similarity metric, such as cosine similarity, in the embedding space $\phi(\cdot)$.

The denoising model is then conditioned not only on the noisy latent z_t and timestep t , but also on the retrieved support set $\{\phi(y) \mid y \in \xi_k(x, D)\}$. The denoising function becomes:

$$\epsilon_\theta(z_t, t, \{\phi(y)\}), \quad (7)$$

where conditioning is typically implemented using cross-attention layers that attend to the retrieved features during noise prediction [8].

The training objective follows the denoising loss paradigm, extended to include retrieval conditioning:

$$\mathcal{L}_{\text{RDM}} = \mathbb{E}_{x, \epsilon, t} \left[\left\| \epsilon - \epsilon_\theta(z_t, t, \{\phi(y) \mid y \in \xi_k(x, D)\}) \right\|^2 \right]. \quad (8)$$

This formulation enables the model to ground its generation in real, semantically similar samples, which is particularly beneficial in data-scarce regimes or when fine control over the output is desired. Unlike purely parametric approaches, RDMs flexibly adapt to new domains by querying from an updated external memory without retraining the entire model.

C. Prototype Learning in Diffusion Models

Prototype-based learning has become a cornerstone of few-shot learning, where the objective is to generalize to novel classes from only a few labeled examples. One of the most influential approaches in this domain is the Prototypical Network (ProtoNet) [20], which embeds both support and query samples into a common metric space and performs classification based on distances to class prototypes.

Given a set of K support examples $\{x_{c,k}\}_{k=1}^K$ for a class c , a class prototype $z_c \in \mathbb{R}^d$ is computed as the mean of their embeddings under a shared encoder f_ϕ :

$$z_c = \frac{1}{K} \sum_{k=1}^K f_\phi(x_{c,k}), \quad (9)$$

where f_ϕ is typically a neural network trained to produce discriminative embeddings. A query sample x_q is classified by computing the softmax over negative distances to each prototype:

$$p(y = c \mid x_q) = \frac{\exp(-d(f_\phi(x_q), z_c))}{\sum_{c'} \exp(-d(f_\phi(x_q), z_{c'}))}, \quad (10)$$

where $d(\cdot, \cdot)$ is usually the squared Euclidean distance in the embedding space. In the context of diffusion models, class prototypes can be leveraged to guide the generative process, especially in scenarios where class-conditioning is required with limited labeled data. Instead of conditioning the diffusion process on textual prompts or class labels alone, prototype-guided diffusion injects semantic structure directly from few-shot support examples.

Let z_c denote the prototype for the target class c , and let x_t be a noisy sample at timestep t . The denoising model can be conditioned on z_c to produce a prototype-guided noise estimate $\epsilon_\theta(x_t, t, z_c)$. Following the classifier-free guidance strategy [21], the final guided noise estimate is computed as:

$$\epsilon_{\text{guided}}(x_t, t) = (1 + s) \cdot \epsilon_\theta(x_t, t, z_c) - s \cdot \epsilon_\theta(x_t, t), \quad (11)$$

where $\epsilon_\theta(x_t, t)$ is the unconditional noise prediction, and $s \geq 0$ is a guidance scale parameter controlling the strength of conditioning. When $s = 0$, the model generates unconditionally; larger values of s encourage outputs more aligned with the class prototype.

This formulation enables the diffusion model to generate samples that are consistent with the semantic identity of a class, even in few-shot or low-resource regimes. Moreover, prototype guidance introduces minimal overhead while providing strong inductive bias via non-parametric, data-driven class priors.

IV. METHOD

The Prototype Diffusion Model (PDM) is a generative model that leverages prototype learning to condition the denoising process in diffusion models. Unlike previous methods such as ProtoDiffusion, which rely on labeled datasets for supervised prototype assignment, PDM is trained in a fully unsupervised manner. This allows the model to discover and utilize semantic prototypes without the need for

annotations, making it particularly well-suited for unlabeled data.

The model is composed of two jointly trained neural networks. The first, denoted f_ϕ , is a convolutional neural network responsible for feature extraction. Given an input image $x \in \mathbb{R}^{H \times W \times C}$, it produces a latent representation:

$$\hat{x} = f_\phi(x), \quad \hat{x} \in \mathbb{R}^D \quad (12)$$

A set of K prototypes $\{e_1, \dots, e_K\} \subset \mathbb{R}^D$ is maintained as learnable parameters, randomly initialized at the start of training. For each image x , the closest prototype is selected based on Euclidean distance in the latent space:

$$e_x = \arg \min_{e_i} \|f_\phi(x) - e_i\|_2 \quad (13)$$

The second component of PDM is the denoising network f_θ , implemented as a U-Net [22], which takes as input a noisy image and is conditioned on the selected prototype. To incorporate the prototype into the U-Net, cross-attention layers are added such that the prototype e_x acts as both key and value, while the query originates from the output of the previous block processing the noisy image. This enables the network to guide the denoising process using the most relevant semantic concept.

Following the standard diffusion framework, Gaussian noise is added to the input image over T steps using the forward process:

$$\tilde{x}_t = \sqrt{\bar{\alpha}_t}x + \sqrt{1 - \bar{\alpha}_t}\epsilon, \quad \epsilon \sim \mathcal{N}(0, I) \quad (14)$$

At each time step t , the denoising network receives \tilde{x}_t , the selected prototype e_x , and a time embedding $\gamma(t)$. The prototype is enriched with this temporal information before being passed to the attention mechanism:

$$\hat{e} = f_\theta(\tilde{x}_t, e_x + \gamma(t)) \quad (15)$$

The training objective of PDM includes several loss components. First, a contrastive loss encourages the feature extractor f_ϕ to bring the latent representation $f_\phi(x)$ close to its associated prototype while pushing it away from others:

$$\mathcal{L}_{\text{contrastive}} = -\log \left(\frac{\exp(-\tau \|f_\phi(x) - e_x\|_2^2)}{\sum_{k=1}^K \exp(-\tau \|f_\phi(x) - e_k\|_2^2)} \right) \quad (16)$$

In addition, an alignment loss directly penalizes the squared Euclidean distance between the image representation and the selected prototype:

$$\mathcal{L}_{\text{align}} = \|f_\phi(x) - e_x\|_2^2 \quad (17)$$

To ensure that the learned prototypes are diverse and semantically meaningful, a compactness regularization term is introduced. This term penalizes high similarity between different prototypes using cosine similarity:

$$\mathcal{L}_{\text{compact}} = \sum_{k \neq k'} \text{sim}(e_k, e_{k'}) \quad (18)$$

where $\text{sim}(e_k, e_{k'})$ denotes the cosine similarity between prototypes e_k and $e_{k'}$. This encourages the prototypes to capture distinct concepts rather than collapsing into similar

representations.

The diffusion objective follows the standard DDPM loss, measuring the mean squared error between the predicted noise and the true noise added at each time step:

$$\mathcal{L}_{\text{diff}} = \mathbb{E}_{x, t, \epsilon} \left[\|\epsilon - f_\theta(\tilde{x}_t, e_x + \gamma(t))\|_2^2 \right] \quad (19)$$

The overall training loss for PDM combines all components:

$$\mathcal{L}_{\text{PDM}} = \mathcal{L}_{\text{diff}} + \mathcal{L}_{\text{contrastive}} + \mathcal{L}_{\text{align}} + \mathcal{L}_{\text{compact}} \quad (20)$$

The training procedure for the Prototype Diffusion Model is detailed in Algorithm 1.

Algorithm 1: Training Prototype Diffusion Model (PDM)

Input: Dataset $\mathcal{D} = \{x_i\}_{i=1}^N$, number of prototypes K , noise schedule $\{\alpha_t\}_{t=1}^T$, weights τ, α, β
Output: Trained networks f_ϕ, f_θ , and prototypes $\{e_1, \dots, e_K\}$

1 Initialize feature extractor f_ϕ , denoiser f_θ , and prototypes $\{e_1, \dots, e_K\} \subset \mathbb{R}^D$;
2 **foreach** minibatch $\{x_1, \dots, x_B\} \subset \mathcal{D}$ **do**
3 **foreach** $x_i \in \{x_1, \dots, x_B\}$ **do** // Feature encoding and prototype assignment
4 Compute $\hat{x}_i = f_\phi(x_i)$;
5 Select prototype: $e_{x_i} = \arg \min_{e_k} \|\hat{x}_i - e_k\|_2$;
6 Sample $t \sim \mathcal{U}\{1, T\}$, $\epsilon \sim \mathcal{N}(0, I)$;
7 Compute $\bar{\alpha}_t = \prod_{s=1}^t \alpha_s$;
8 Compute $\tilde{x}_i = \sqrt{\bar{\alpha}_t}x_i + \sqrt{1 - \bar{\alpha}_t}\epsilon$;
9 Predict $\hat{e}_i = f_\theta(\tilde{x}_i, e_{x_i} + \gamma(t))$;
10 Compute loss terms:
11 $\mathcal{L}_{\text{contrastive}} = -\frac{1}{B} \sum_{i=1}^B \log \left(\frac{\exp(-\tau \|\hat{x}_i - e_{x_i}\|_2^2)}{\sum_{k=1}^K \exp(-\tau \|\hat{x}_i - e_k\|_2^2)} \right)$;
12 $\mathcal{L}_{\text{align}} = \frac{1}{B} \sum_{i=1}^B \|\hat{x}_i - e_{x_i}\|_2^2$;
13 $\mathcal{L}_{\text{compact}} = \beta \sum_{k \neq k'} \text{sim}(e_k, e_{k'})$;
14 $\mathcal{L}_{\text{diff}} = \frac{1}{B} \sum_{i=1}^B \|\epsilon_i - \hat{e}_i\|_2^2$;
15 Combine losses:
16 $\mathcal{L}_{\text{PDM}} = \mathcal{L}_{\text{diff}} + \mathcal{L}_{\text{contrastive}} + \alpha \cdot \mathcal{L}_{\text{align}} + \beta \cdot \mathcal{L}_{\text{compact}}$;
17 Update $f_\phi, f_\theta, \{e_k\}$ via gradient descent on \mathcal{L}_{PDM} ;
18 **return** $f_\phi, f_\theta, \{e_k\}_{k=1}^K$;

During inference, PDM supports both conditional and unconditional generation. If an input image is provided, it is passed through f_ϕ to select the most appropriate prototype e_x , which is then used to condition the denoising process. If no image is provided, a prototype is selected at random. The complete inference process is summarized in Algorithm 2.

PDM can be readily adapted to a supervised context in which labeled data is available. We create and refer to this variant as **supervised Diffusion Prototype Model (s-PDM)**. In this case, each class is associated with a fixed prototype. Therefore, during training, prototype selection is unnecessary since the correct prototype is known. Moreover,

Algorithm 2: Inference in Prototype Diffusion Model (PDM)

Input: Prototype set $\{e_1, \dots, e_K\}$, trained feature extractor f_ϕ , denoiser f_θ , optional image x , noise schedule $\{\alpha_t\}_{t=1}^T$

Output: Generated image \hat{x}_0

```

1 if image  $x$  is provided then
2   Compute  $\hat{x} = f_\phi(x)$ ;
3   Select prototype:  $e_x = \arg \min_{e_i} \|\hat{x} - e_i\|_2$ ;
4 else
5   Sample prototype  $e_x \sim \{e_1, \dots, e_K\}$ ;
6 Initialize  $\tilde{x}_T \sim \mathcal{N}(0, I)$ ;
7 for  $t \leftarrow T$  to 1 do // Iterative denoising
8   Compute  $\bar{\alpha}_t = \prod_{s=1}^t \alpha_s$ ;
9   Compute  $\hat{\epsilon}_t = f_\theta(\tilde{x}_t, e_x + \gamma(t))$ ;
10  Compute  $\sigma_t = \sqrt{1 - \bar{\alpha}_t}$ , sample  $z \sim \mathcal{N}(0, I)$ ;
11  Update:
12    
$$\tilde{x}_{t-1} = \frac{1}{\sqrt{\bar{\alpha}_t}} \left( \tilde{x}_t - \frac{1 - \alpha_t}{\sqrt{1 - \bar{\alpha}_t}} \hat{\epsilon}_t \right) + \sigma_t z$$

12 return  $\hat{x}_0 = \tilde{x}_0$ ;

```

the compactness loss $\mathcal{L}_{\text{compact}}$ is no longer needed, as inter-class semantic separation is enforced by the labels themselves. The resulting supervised loss simplifies to:

$$\mathcal{L}_{\text{PDM-supervised}} = \mathcal{L}_{\text{diff}} + \mathcal{L}_{\text{contrastive}} + \mathcal{L}_{\text{align}} \quad (21)$$

The inference procedure remains unchanged, conditioned either on a labeled image or a sampled prototype for unconditional generation. This flexibility allows PDM to operate seamlessly in both supervised and unsupervised settings.

V. EXPERIMENTS

We conduct our experiments on CIFAR-10 [23], STL-10 [24], EuroSAT [25], and Tiny ImageNet [26] datasets using 2 NVIDIA A100 GPUs. Table I summarizes the key characteristics of the datasets, including the number of classes, total number of images, image resolution, and train/test splits.

For the denoiser (U-Net), we use the same compact architecture across all experiments, with a total block configuration of [128, 256, 256, 256] channels for successive downsampling and upsampling stages. Downsampling progressively increases the number of channels while reducing spatial resolution, whereas upsampling mirrors this process to recover the original resolution.

We incorporate the prototypes at the bottleneck, immediately after the final downsampling stage, using an attention mechanism. This design choice is motivated by the fact that the bottleneck captures the highest-level semantic features with the smallest spatial footprint, making it computationally

efficient to attend to prototypes while maximizing their influence on global structure and class-specific semantics. By conditioning the most abstract feature representation on learned prototypes, we guide the generative process toward both semantic fidelity and intra-class consistency without imposing significant computational overhead.

We compare PDM and s-PDM against two relevant baselines. The first is *DDPM*, a standard U-Net-based diffusion model without prototypes, which can be viewed as an ablation of PDM where the prototype mechanism is removed. This comparison highlights that removing prototypes limits performance and that prototype-based conditioning can bring significant improvements. The second is *ProtoDiffusion*, a two-stage method in which prototypes are learned separately, frozen, and then injected into the bottleneck of the U-Net denoiser. While this approach incorporates prototypes, its separate training and freezing strategy make it computationally costly and unable to adapt prototypes to distribution shifts during denoiser training, which can progressively reduce their relevance. Our encoder f_ϕ uses a lightweight CNN with four convolutional layers followed by adaptive average pooling to extract features suitable for prototype learning.

For evaluation, we use three widely adopted generative quality metrics: *Inception Score (IS)* [27], *Fréchet Inception Distance (FID)* [25], and *Kernel Inception Distance (KID)* [28]. The IS measures both the diversity and semantic clarity of generated images by computing the KL divergence between the conditional label distribution predicted by a pretrained Inception network and its marginal distribution; it does not require real target images but relies on the classifier's learned label space. In contrast, FID compares the distribution of real and generated images in the feature space of the Inception network by modeling both as multivariate Gaussians; it explicitly requires real target samples and evaluates how close the generated distribution is to the real one. Similarly, KID compares real and generated images in the Inception feature space but uses the squared Maximum Mean Discrepancy (MMD) with a polynomial kernel instead of Gaussian assumptions; like FID, it requires real target samples, but unlike FID, it is unbiased for a finite number of samples.

A. Comparison of PDM, s-PDM, and Baseline Models on Generative Quality Metrics

Table II shows a comprehensive comparison of generative performance across four datasets using IS, FID, and KID. Our proposed methods, PDM and s-PDM, consistently outperform the baselines DDPM and ProtoDiffusion on most metrics, demonstrating the effectiveness of incorporating prototypes within the diffusion framework.

In particular, s-PDM achieves the best FID and KID scores on all datasets, indicating superior generation quality and distributional alignment with the target data. This improvement can be attributed to the supervised nature of

Dataset	# Classes	# Training Images	# Test Images	Resolution
CIFAR-10	10	50,000	10,000	32 × 32
STL-10	10	5,000	8,000	96 × 96
EuroSAT	10	21,600	5,400	64 × 64
Tiny ImageNet	200	100,000	10,000	64 × 64

TABLE I: Summary of datasets used in our experiments.

Method	CIFAR-10			STL-10			EuroSAT			Tiny ImageNet		
	IS ↑	FID ↓	KID ↓	IS ↑	FID ↓	KID ↓	IS ↑	FID ↓	KID ↓	IS ↑	FID ↓	KID ↓
DDPM	7.12	18.45	0.021	7.85	34.20	0.038	3.75	28.47	0.018	9.05	48.22	0.08
ProtoDiffusion	8.50	11.70	0.009	9.40	22.70	0.015	4.45	15.20	0.010	10.55	31.00	0.04
PDM (ours)	8.35	8.10	0.007	9.25	21.30	0.011	4.40	13.50	0.008	11.20	25.40	0.03
s-PDM (ours)	8.20	6.58	0.004	9.20	20.32	0.007	4.52	11.29	0.005	11.65	23.00	0.02

TABLE II: Quantitative comparison of generative quality across datasets using Inception Score (IS, ↑), Fréchet Inception Distance (FID, ↓), and Kernel Inception Distance (KID, ↓). For all datasets, the number of prototypes used equals the number of classes. Best results per column are in **bold**.

s-PDM: each class is associated with a fixed prototype that directly guides the generation process. As FID and KID explicitly measure the similarity between generated samples and real data distributions, having class-specific prototypes ensures more relevant and accurate sample generation.

On the other hand, IS does not explicitly consider class labels during evaluation, which explains why s-PDM’s IS is sometimes slightly lower than PDM or ProtoDiffusion. PDM, being unsupervised, optimizes to cluster similar images without label guidance, resulting in slightly better IS values that reflect sample diversity but less precise class alignment. This difference is visually supported by Figure 1, where we apply PCA on the output features of f_ϕ and color-code samples by CIFAR-10 classes. The s-PDM clusters show clearer class separation than PDM, highlighting the advantage of supervised prototype learning in structuring the latent space according to semantic categories. In contrast, PDM’s parameters are randomly initialized and updated without class supervision, focusing solely on grouping similar images regardless of class labels.

Overall, these results confirm that supervised prototype guidance in s-PDM leads to more semantically meaningful and distributionally faithful generation, improving key metrics sensitive to sample quality and fidelity.

B. Ablation Study: Number of Prototypes in PDM

To evaluate the sensitivity of PDM to the number of prototypes, we vary this hyperparameter while keeping all other settings fixed. Since CIFAR-10 has 10 classes, the default configuration uses 10 prototypes (one per class). We investigate smaller values (3, 5, 7) and larger values (13, 15, 20) to observe how performance changes when the prototype count deviates from the number of classes.

Table III shows that reducing the number of prototypes below the number of classes leads to a clear drop in performance across all metrics. For example, decreasing from 10 to 3 prototypes reduces IS from 8.35 to 7.50 and increases FID from 8.10 to 11.90, indicating lower generation quality and poorer alignment with the real

# Prototypes	IS ↑	FID ↓	KID ↓
3	7.50	11.90	0.010
5	7.85	10.20	0.009
7	8.10	9.10	0.008
10	8.35	8.10	0.007
13	8.42	7.95	0.006
15	8.48	7.85	0.006
20	8.20	7.70	0.006

TABLE III: Effect of varying the number of prototypes in PDM on CIFAR-10. Performance is measured using Inception Score (IS), Fréchet Inception Distance (FID), and Kernel Inception Distance (KID).

data distribution. This degradation occurs because fewer prototypes cannot represent the semantic diversity of the dataset, forcing multiple classes to share a prototype and thereby merging distinct modes in the data distribution. When increasing the number of prototypes beyond 10, IS improves slightly up to 15 prototypes, reflecting a modest gain in sample diversity. However, FID and KID also decrease slightly, suggesting better fidelity and distributional alignment. At 20 prototypes, IS drops again, likely due to over-fragmentation of the latent space: too many prototypes may split coherent clusters, leading to redundant or less meaningful centroids without adding new semantic structure. These results are highly relevant because they demonstrate the importance of matching the number of prototypes to the inherent class structure of the dataset. The optimal setting (10 prototypes for CIFAR-10) aligns naturally with the number of classes, balancing diversity (high IS) with fidelity (low FID and KID). This finding supports the idea that prototypes in PDM should reflect the dataset’s underlying semantic granularity rather than being arbitrarily chosen.

C. Qualitative Results: Sample Generations

After training for 500 epochs, we generate 8×8 image grids by sampling from the model using Algorithm 2 with $T = 1000$ denoising steps. For each generation, prototypes are selected randomly from the learned set. Figure 2

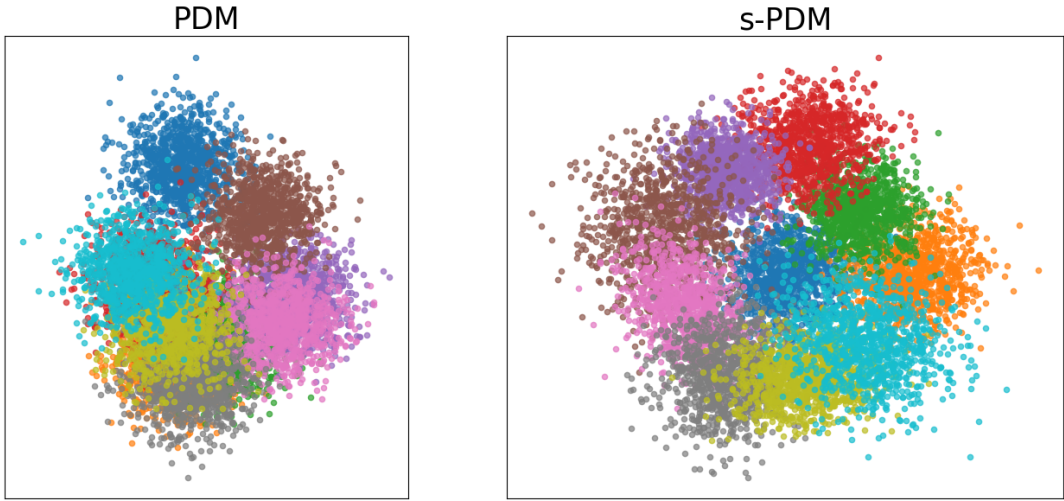


Fig. 1: PCA visualization of the output features of f_ϕ colored by CIFAR-10 classes, showing cluster separation for PDM and s-PDM.

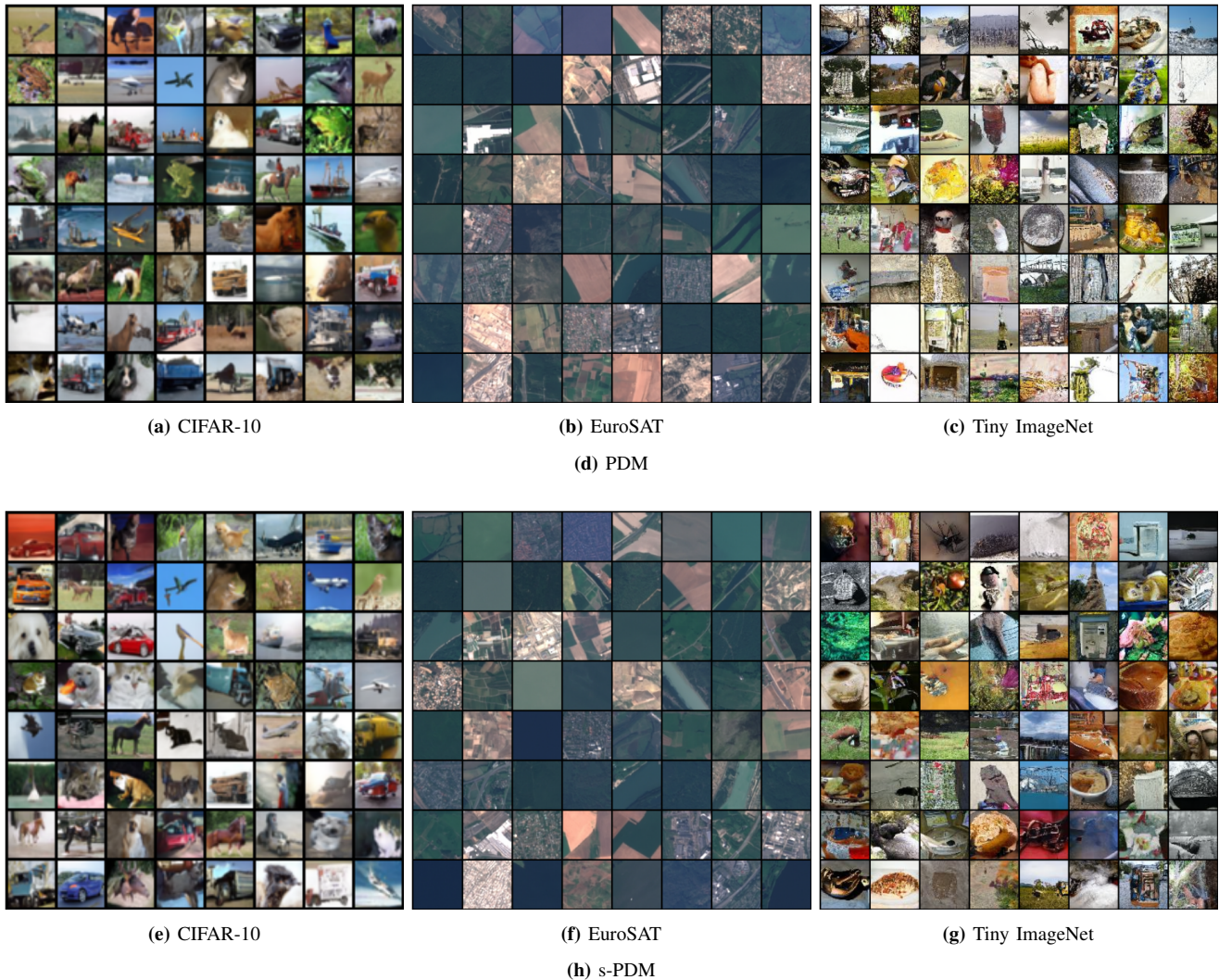


Fig. 2: Qualitative comparison of generated samples from PDM (top) and s-PDM (bottom) across CIFAR-10, EuroSAT, and Tiny ImageNet. Each subfigure displays an 8×8 grid of randomly generated images obtained after 500 training epochs using $T = 1000$ denoising steps. While s-PDM produces slightly sharper and more class-aligned samples, PDM still achieves visually plausible generations without supervision.

presents qualitative examples on CIFAR-10, EuroSAT, and Tiny ImageNet for both PDM (unsupervised) and s-PDM (supervised).

Despite s-PDM achieving superior quantitative scores (Tables II), the visual fidelity of PDM remains competitive. The unsupervised variant captures coherent structures, realistic textures, and reasonable semantic consistency, even without explicit label guidance. This observation suggests that, in many practical scenarios where labeled data is limited or unavailable, an unsupervised prototype diffusion approach can still yield perceptually compelling generations while maintaining reduced training complexity.

VI. CONCLUSION

VII. CONCLUSION AND FUTURE WORK

We introduced the *Prototype Diffusion Model* (PDM) and its supervised variant *s-PDM*, which integrate prototype learning directly into diffusion training. PDM learns prototypes online without labels, offering strong semantic grounding and competitive visual quality while avoiding external retrieval systems and large memory banks. In contrast, s-PDM leverages class labels to attach fixed prototypes, yielding the best quantitative results (e.g., lower FID/KID) but requiring annotations. Our experiments show that prototype-guided conditioning is effective in both regimes: s-PDM delivers state-of-the-art fidelity with labels, while PDM remains a practical, label-free alternative with compelling qualitative results and reduced overhead. Ablations on prototype count further validate that aligning prototype granularity with dataset semantics is key to performance.

Future work will extend prototype-guided conditioning to **text-to-image generation** by learning a shared multimodal space for language-driven prototype selection and composition. We also plan to explore semi- and weakly supervised variants (bridging PDM and s-PDM), hierarchical/compositional prototypes for complex scenes, and online adaptation to distribution shifts to maintain prototype relevance during long-term training and deployment.

REFERENCES

- [1] J. Ho, A. Jain, and P. Abbeel, “Denoising diffusion probabilistic models,” *Advances in neural information processing systems*, vol. 33, pp. 6840–6851, 2020.
- [2] F. Mazé and F. Ahmed, “Diffusion models beat gans on topology optimization,” in *Proceedings of the AAAI conference on artificial intelligence*, vol. 37, pp. 9108–9116, 2023.
- [3] P. Dhariwal and A. Nichol, “Diffusion models beat gans on image synthesis,” *Advances in neural information processing systems*, vol. 34, pp. 8780–8794, 2021.
- [4] J. Song, C. Meng, and S. Ermon, “Denoising diffusion implicit models,” in *International Conference on Learning Representations (ICLR)*, 2021.
- [5] C. Saharia, W. Chan, S. Saxena, L. Li, J. Whang, E. L. Denton, K. Ghasemipour, R. Gontijo Lopes, B. Karagol Ayan, T. Salimans, *et al.*, “Photorealistic text-to-image diffusion models with deep language understanding,” *Advances in neural information processing systems*, vol. 35, pp. 36479–36494, 2022.
- [6] A. Lugmayr, M. Danelljan, A. Romero, F. Yu, R. Timofte, and L. Van Gool, “Repaint: Inpainting using denoising diffusion probabilistic models,” in *Proceedings of the IEEE/CVF conference on computer vision and pattern recognition*, pp. 11461–11471, 2022.
- [7] Y. Zhou, B. Liu, Y. Zhu, X. Yang, C. Chen, and J. Xu, “Shifted diffusion for text-to-image generation,” in *Proceedings of the IEEE/CVF conference on computer vision and pattern recognition*, pp. 10157–10166, 2023.
- [8] R. Rombach, A. Blattmann, D. Lorenz, P. Esser, and B. Ommer, “High-resolution image synthesis with latent diffusion models,” in *Proceedings of the IEEE/CVF conference on computer vision and pattern recognition*, pp. 10684–10695, 2022.
- [9] A. Blattmann, R. Rombach, K. Oktay, J. Müller, and B. Ommer, “Retrieval-augmented diffusion models,” *Advances in Neural Information Processing Systems*, vol. 35, pp. 15309–15324, 2022.
- [10] A. Radford, J. W. Kim, C. Hallacy, A. Ramesh, G. Goh, S. Agarwal, G. Sastry, A. Askell, P. Mishkin, J. Clark, *et al.*, “Learning transferable visual models from natural language supervision,” in *International conference on machine learning*, pp. 8748–8763, PMLR, 2021.
- [11] G. Baykal, H. F. Karagoz, T. Binhuraib, and G. Unal, “Protodiffusion: Classifier-free diffusion guidance with prototype learning,” in *Asian Conference on Machine Learning*, pp. 106–120, PMLR, 2024.
- [12] Y. Song, P. Dhariwal, M. Chen, and I. Sutskever, “Consistency models,” in *Proceedings of the 40th International Conference on Machine Learning* (A. Krause, E. Brunskill, K. Cho, B. Engelhardt, S. Sabato, and J. Scarlett, eds.), vol. 202 of *Proceedings of Machine Learning Research*, pp. 32211–32252, PMLR, 23–29 Jul 2023.
- [13] D. Podell, Z. English, K. Lacey, A. Blattmann, T. Dockhorn, J. Müller, J. Penna, and R. Rombach, “SDXL: improving latent diffusion models for high-resolution image synthesis,” in *The Twelfth International Conference on Learning Representations, ICLR 2024, Vienna, Austria, May 7-11, 2024*, 2024.
- [14] Z. Huang, L. Yang, X. Zhou, C. Qin, Y. Yu, X. Zheng, Z. Zhou, W. Zhang, Y. Wang, and W. Yang, “Interaction-based retrieval-augmented diffusion models for protein-specific 3d molecule generation,” in *Forty-first International Conference on Machine Learning*, 2024.
- [15] Y. Du, Z. Xiao, S. Liao, and C. Snoek, “Protodiff: Learning to learn prototypical networks by task-guided diffusion,” in *Advances in Neural Information Processing Systems 36: Annual Conference on Neural Information Processing Systems 2023, NeurIPS 2023, New Orleans, LA, USA, December 10 - 16, 2023*, 2023.
- [16] K. Doan, Q. Tran, T. L. Tran, T. Nguyen, D. Phung, and T. Le, “Class-prototype conditional diffusion model with gradient projection for continual learning,” *arXiv preprint arXiv:2312.06710*, 2023.
- [17] J. Sohl-Dickstein, E. Weiss, N. Maheswaranathan, and S. Ganguli, “Deep unsupervised learning using nonequilibrium thermodynamics,” in *International conference on machine learning*, pp. 2256–2265, pmlr, 2015.
- [18] Z. Hu, A. Iscen, C. Sun, Z. Wang, K.-W. Chang, Y. Sun, C. Schmid, D. A. Ross, and A. Fathi, “Reveal: Retrieval-augmented visual-language pre-training with multi-source multimodal knowledge memory,” in *Proceedings of the IEEE/CVF conference on computer vision and pattern recognition*, pp. 23369–23379, 2023.
- [19] P. Esser, R. Rombach, and B. Ommer, “Taming transformers for high-resolution image synthesis,” in *Proceedings of the IEEE/CVF conference on computer vision and pattern recognition*, pp. 12873–12883, 2021.
- [20] J. Snell, K. Swersky, and R. Zemel, “Prototypical networks for few-shot learning,” *Advances in neural information processing systems*, vol. 30, 2017.
- [21] J. Ho and T. Salimans, “Classifier-free diffusion guidance,” *arXiv preprint arXiv:2207.12598*, 2022.
- [22] O. Ronneberger, P. Fischer, and T. Brox, “U-net: Convolutional networks for biomedical image segmentation,” in *Medical image computing and computer-assisted intervention–MICCAI 2015: 18th international conference, Munich, Germany, October 5-9, 2015, proceedings, part III 18*, pp. 234–241, Springer, 2015.
- [23] A. Krizhevsky, G. Hinton, *et al.*, “Learning multiple layers of features from tiny images,” 2009.
- [24] A. Coates, A. Ng, and H. Lee, “An analysis of single-layer networks in unsupervised feature learning,” in *Proceedings of the fourteenth international conference on artificial intelligence and statistics*, pp. 215–223, JMLR Workshop and Conference Proceedings, 2011.

- [25] P. Helber, B. Bischke, A. Dengel, and D. Borth, “Eurosat: A novel dataset and deep learning benchmark for land use and land cover classification,” *IEEE Journal of Selected Topics in Applied Earth Observations and Remote Sensing*, vol. 12, no. 7, pp. 2217–2226, 2019.
- [26] Y. Le and X. Yang, “Tiny imagenet visual recognition challenge,” *CS 231N*, vol. 7, no. 7, p. 3, 2015.
- [27] T. Salimans, I. Goodfellow, W. Zaremba, V. Cheung, A. Radford, and X. Chen, “Improved techniques for training gans,” in *Advances in neural information processing systems*, vol. 29, 2016.
- [28] M. Binkowski, D. Sutherland, M. Arbel, and A. Gretton, “Demystifying mmd gans,” in *International Conference on Learning Representations (ICLR)*, 2018.